SYNTHESIS, SPECTROSCOPIC AND BIOLOGICAL INVASTIGATION OF FE(II), CO(II), NI(II), RU(III), RH(III), IR(III), CR(III), PD(II), CU(II) AND MN(II) COMPLEXES WITH BENZILMONOXIMEHYDRAZIDE-*O*-CHLOROBENZALDEHYDE

Sharad Sankhe[1*], Krupali Shah[2]

Abstract.
A host of new Fe(II), Co(II), Ni(II), Ru(III), Rh(III), Ir(III), Cr(III), Pd(II), Cu(II) and Mn(II) complexes with benzilmonoximehydrazide-*o*-chlorobenzaldehyde (HBMH*o*CB) ligand have been prepared and characterised through physicochemical and analytical data. The electronic and magnetic moment data studies classify the reported as 5 or 6-membered coordinated geometry. The FT(IR) spectra scrutiny between the HBMH*o*CB ligand and its bivalent and trivalent metal complexes and in analogy with the crystal structure analysis indicate that the HBMH*o*CB ligand exercises neutral bidentate (N, N) behaviour through azomethine and oximino group bind with central bivalent as well as trivalent metal ions.

Keywords: Benzilmonoximehydrazide, *o*-Chlorobenzaldehyde, Electronic spectra, Magnetic moment

[1*]Professor, Department of Chemistry, Patkar-Varde College, Goregaon West, Mumbai-62, India.
[2]PhD scholar, Department of Chemistry, Patkar-Varde College, Goregaon West, Mumbai-62, India.

***Corresponding Author:** Sharad Sankhe
*Professor, Department of Chemistry, Patkar-Varde College, Goregaon West, Mumbai-62, India.

DOI: 10.48047/ecb/2023.12.si5a.0318

Introduction:

Due to their numerous bonding mechanisms, oximes are crucial in advancing transition metal coordination chemistry. Chelating compounds known as benzolmonoximes are frequently employed in analytical and extractive chemistry. Atomic absorption spectroscopy, for instance, has been used to determine the amount of copper in a solution based on its benzilmonoxime complex[1-5]. It is a well-known extractant for molybdenum, tungsten, and vanadium, as well as for the microgram-level detection of cobalt. Many of the described benzilmonoximates exhibit intriguing stereochemistry. Due to their biological activity and semi-conducting qualities, benzilmonoximes are particularly interesting[3]. The importance of benzilmonoximes has been appreciated particularly in relevance to the coordination chemistry, which has their transition and inner transition metal complexes[1-5]. The biological activity of benzilmonoxime and its various derivatives is well-acclaimed; Benzilmonoximehydrazide, for example, has a powerful stimulating action on the central nervous systems and is found extensively used as a respiratory stimulant[6-9]. Given this and our continuing interest in the synthesis of new benzilmonoximes, the present communication reports the preparation and characterisation of Fe(II), Co(II), Ni(II), Ru(III), Rh(III), Ir(III), Cr(III), Pd(II), Cu(II) and Mn(II) complexes with benzilmonoximehydrazide-*o*-chlorobenzaldehyde (HBMH*o*CB) ligand.

1. Experimental:

All the solvents and chemicals were used of AR quality without further purification.

The HBMH*o*CB is with Fe(II), Co(II), Ni(II), Ru(III), Rh(III), Ir(III), Cr(III), Pd(II), Cu(II) and Mn(II) complexes were analysed at Thermo Finning FLASH -1112 series analyser. The Fe(II), Co(II), Ni(II), Ru(III), Rh(III), Ir(III), Cr(III), Pd(II), Cu(II) and Mn(II) metal contents to as determine gravimetrically. The trivalent metal complex's magnetic susceptibility measurements were measured on a Gory balance using $[Co(Hg(SCN)_4]$ as a standard at 301K. The UV visible spectra recorded on JASCO uv-visible spectrophotometer and FT(IR) spectra were recorded on a Perkin-Elmer spectrum-100 model FT-IR spectrophotometer in the solid state.

1.1. Synthesis of HBMH*o*CB Ligand:

To a solution of benzilmonoximehydrazide (23.9 g, 0.100mol) in warm methanol (100 mL) was added a methanolic solution of *o*-chlorobenzladehyde (17.50 mg, 0.0125 mmol) and conc. HCl (5ml). The reaction mixture was refluxed for 3 hours. When the solution was cooled, a yellow precipitate was formed, filtered off and washed with hot water. The crude material was then recrystallised from methanol to give (27.04 g, 74.89%) pure HBMH*o*CB.

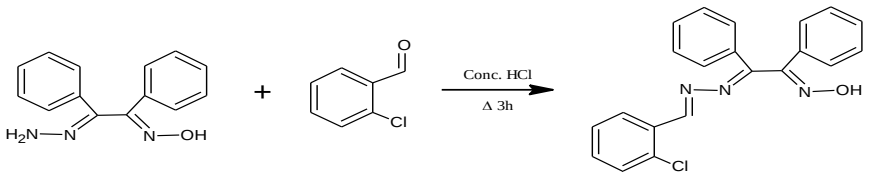

Figure-1: Reaction scheme of HBMH*o*CB ligand

1.2. Synthesis of transition metal complexes:

An aq. Solution of metal (II/III) chloride (5mmol) was added to the ethanol solution of HBMH*o*CB ligand (10mmol), and pH was adjusted to 7. The final reaction mixture was refluxed in a water bath for 6-9h and cooled to 28°C; the solid-coloured compounds were separated by filtration and washed with hot distilled water dried over silica gel at room temperature.

Antibacterial activity:

The paper disc diffusion method was used to evaluate the antibacterial efficacy of HBMH*o*CB and its complexes. Strains of G(+) Staphylococcus aureus and G(-) Escherichia coli, Klebsiella pneumoniae, Pseudomonas aeruginosa, and Staphylococcus epidermidis were selected. After incubation for 24 hours, the diameter of the growth-inhibitory zone around the disc was calculated. Each treatment included four replicates, and the values shown are the mean average.

2. Results and Discussion:

The reaction of metal (II/III) chloride salts with three equivalents of the HBMH*o*CB ligand in alcohol affords the solid compounds with varying colours better yield at 28-30°C. The reaction route is stated as follows:

$MCl_3 + 3HBHoCB \rightarrow M(BMHoCB)_3 + 3HCl$ and

$MCl_2 + 2HBHoCB \rightarrow M(BMHoCB)_2 + 2HCl$

All prepared metal complexes confirm the general composition $[M(BMHoCB)_3]$ for Ru(III), Rh(III),

Ir(III), Cr(III), and [M(BMH*o*CB)$_2$] for Fe(II), Co(II), Ni(II), Pd(II), Cu(II) and Mn(II) complexes as ascertained[10-12] from physicochemical and analytical data (**Table-1**). The prepared metal complexes molar conductance values (**Table-1**) recorded in nitrobenzene (Λ_m0.53-3.68Ω^{-1}cm^{2}mol) indicate the non-electrolytic nature of all complexes[13-14].

Table-1: Analytical and physical data of the HBMH*o*CB ligand and its metal complexes

Compound	Colour	Yield %	M.P. / Dec. point°C	Elemental Analysis						Magnetic Moments (B.M.)	Electrical Conductance 10^{-3} M(in NB) mhos
				% M Found (Calcd)	% C Found (Calcd)	% H Found (Calcd)	% N Found (Calcd)	% O Found (Calcd)	Cl% Found (Calcd)		
HBMH*o*CB	Yellow	84.54	198	-	69.59 (69.71)	4.43 (4.46)	11.60 (11.61)	4.41 (4.42)	9.80 (9.80)	-	-
[Fe(BMH*o*CB)$_2$]	Blue	81.19	211	7.12 (7.20)	64.91 (64.96)	3.80 (3.87)	10.61 (10.83)	4.09 (4.12)	9.15 (9.15)	4.82	3.68
[Co(BMH*o*CB)$_2$]	Brown	80.00	213	7.29 (7.57)	64.58 (64.70)	3.65 (3.85)	10.77 (10.78)	4.03 (4.11)	9.03 (9.11)	4.89	0.53
[Ni(BMH*o*CB)$_2$]	Green	78.90	218	7.48 (7.54)	64.47 (64.72)	3.59 (3.85)	10.67 (10.79)	3.78 (3.85)	9.10 (9.12)	3.09	0.89
[Pd(BMH*o*CB)$_2$]	Brown	84.63	213	12.44 (12.83)	60.89 (61.02)	3.51 (3.63)	10.08 (10.17)	3.51 (3.87)	8.48 (8.60)	-	1.99
[Cu(BMH*o*CB)$_2$]	Green	77.64	221	7.94 (8.11)	62.11 (62.32)	3.58 (3.83)	10.19 (10.72)	4.05 (4.08)	9.00 (9.05)	1.98	2.79
[Rh(BMH*o*CB)$_3$]	Brown	80.99	219	8.17 (8.70)	63.91 (63.91)	3.74 (3.80)	10.60 (10.65)	4.02 (4.06)	9.01 (9.00)	2.03	4.49
[Mn(BMH*o*CB)$_2$]	Brown	78.96	214	9.10 (9.16)	64.86 (65.04)	3.86 (3.87)	10.68 (10.84)	4.09 (4.13)	9.15 (9.16)	5.61	1.33
[Ru(BMH*o*CB)$_3$]	Red	76.21	218	8.51 (8.55)	63.90 (64.01)	3.59 (3.81)	10.37 (10.67)	4.03 (4.06)	9.00 (9.02)	3.60	1.12
[Cr(BMH*o*CB)$_3$]	Green	82.98	213	4.55 (4.59)	66.69 (66.78)	3.91 (3.97)	11.12 (11.13)	4.21 (4.24)	11.08 (11.13)	4.35	2.38
[Ir(BMH*o*CB)$_3$]	Brown	79.99	225	15.03 (15.09)	59.29 (59.43)	3.45 (3.54)	9.33 (9.91)	3.72 (3.77)	8.30 (8.37)	1.83	1.55

2.1. Electronic absorption spectra and Magnetic moments:

In chloroform solvent, the electronic spectra of transition metal complexes of HBMH*o*CB ligand are obtained, and the band assignment is displayed in **Table-2.** The energy of the metal *d* orbital, degeneracy, and distribution of electrons all affect the electronic spectrum. The geometry of the complex, the amount and type of ligands, and the metal's oxidation state all impact these characteristics. In the electronic spectra of the Fe(II) complex, which is attributed to the $^5T_{2g}$–^5E_g transition and is consistent with octahedral geometry[15], just one broadband is seen at 613nm.

The magnetic moment of the cobalt(II) complex is 4.89 BM, which corresponds to three unpaired electrons (Table-1). Co(II) complex's electronic spectra show absorption in the ranges of 890 (ε=91mole^{-1}cm^{-1}), 696 (ε=547 mole^{-1}cm^{-1}), and 550nm (ε=938 mole^{-1}cm^{-1}), which is typical of an octahedral geometry[16–19]. The transitions $^4T_{1g}(F) \rightarrow {}^4T_{2g}(F)$ (ν_1), $^4T_{1g} \rightarrow {}^4T_{2g}$ (ν_2), $^4T_{1g}(F) \rightarrow {}^4T_{2g}(P)$ (ν_3), respectively, may be attributed to the bands. The magnetic moment of the Ni(II) complex at room temperature is 3.09 BM. This number is consistent with a high spin configuration and indicates that the complex's Ni(II) ion is surrounded by an octahedral environment[20]. The complex's electronic spectra show three absorption bands in the range of 978 nm (ε= 9 mole^{-1}cm^{-1}), 685 nm (ε= 62 mole^{-1}cm^{-1}), and 530 nm (ε= 657 mole^{-1}cm^{-1}). According to an analysis of these bands, the complex may have D_{4h} symmetry and an octahedral geometry. Ni(II) exists in the ground state 3A2g in octahedral coordination. The three spin-allowed transitions[21], $^3A_{2g}(F) \rightarrow {}^3T_{2g}(F)$ (ν_1), $^3A_{2g}(F) \rightarrow {}^3T_{1g}(F)$ (ν_2) and $^3A_{2g}(F) \rightarrow {}^3T_{1g}(P)$ (ν_3), may thus be attributed to these bands, respectively. This supports an octahedral geometry. Due to the n-π * and $\pi - \pi^*$ transitions, the Pd(II) complex's electronic spectrum contained bands in the 326-245 nm range. The overlap of the low energy $\pi \rightarrow \pi^*$ transitions, which are primarily concentrated inside the azomethine group, and the LMCT transitions from the lone pairs of the oximino donor to Pd (II), led to the less intense and broad bands at 326 and 245 nm in the spectrum of the Pd(II) complex[22].

The Cu(II) complex's magnetic moment measurement at room temperature is 1.98 BM,

equal to one unpaired electron[23,24]. The electronic spectra of the six-coordinate copper complex have absorption bands in the ranges of 975nm (ε=12 $mole^{-1}cm^{-1}$), 690nm (ε=103 $mole^{-1}cm^{-1}$), and 475nm (ε=196 $mole^{-1}cm^{-1}$). These bands could be categorized as one of the three spin[25] permitted transitions listed below: These transitions, $^2B_{1g} \rightarrow {}^2A_{1g}(d_{x2-y2} \rightarrow d^2_z)$ (ν_1), $^2B_{1g} \rightarrow {}^2B_{2g}(d_{x2-y2} \rightarrow d_{zy})$ (ν_2) and $^2B_{1g} \rightarrow {}^2E_g(d_{x2-y2} \rightarrow d_{zy}, d_{yz})$ (ν_3) point to D_{4h} symmetry. The quantity of the tetragonal distortion brought on by the ligand field and the Jahn-Teller distortion effect will determine the order of the energy levels.

The electronic spectrum of [Ru(BMH*o*CB)$_3$] complex is located in bands at 625, 430 and 321nm, which are assigned as $^2T_{2g} \rightarrow {}^4T_{1g}$, $^2T_{2g} \rightarrow {}^4T_{2g}$, and $^2T_{2g} \rightarrow {}^2A_{2g}$, $^2T_{1g}$ transitions respectively[26-27]. The [Rh(BMH*o*CB)$_3$] complex electronic spectrum exhibited bands at 550, 502 and 425nm due to $^1A_{1g} \rightarrow {}^3T_{1g}$, $^1A_{1g} \rightarrow {}^1T_{1g}$ and $^1A_{1g} \rightarrow {}^1T_{2g}$ transitions, respectively, for octahedral Rh(III) complex[28-29]. This observation confirms by the observed magnetic moment at 2.03 B.M.

The electronic absorption spectrum of Ir(III) complex absorbs bands at 642, 470 and 391nm, which may be assigned to the $^1A_{1g} \rightarrow {}^3T_{1g}$, $^2T_{2g} \rightarrow {}^4T_{2g}$, and $^2T_{2g} \rightarrow {}^2A_{2g}$ transitions, respectively[30-32]. At 4.35 BM, the magnetic moment of the chromium(III) complex was discovered. The chromium (III) complex's electronic spectrum has 984, 761, 570, 365, and 283nm bands. However, it is possible to understand these spectral bands in terms of the six coordinated environments surrounding the metal atom[33]. Weak absorption bands at 560 (ν_1), 399 (ν_2), 345 (ν_3), and 312nm (ν_4) of the Mn(II) complex's electronic spectra (**Table-2**) are indicative of the octahedral geometry[34]. These bands can each be classified as $^6A_{1g} \rightarrow {}^4T_{1g}$ (^{4}G), $^6A_{1g} \rightarrow {}^4E_g$ (^{4}G), $^4A_{1g}$ (^{4}G) (10B+5C), $^6A_{1g} \rightarrow {}^4E_g$ (^{4}D), (17B+5C), $^6A_{1g} \rightarrow {}^4T_{1g}$ (^{4}P) transitions respectively.

Table-2: Electronic absorption spectral data of HBMHoCB ligand and its Ln(III) metal complexes

Compound	**λnm**	**ε (dm^3/mol/cm)**	**Transition**
HBMH*o*CB	322	8745	$\pi \rightarrow \pi^*$
	253	9054	$\pi \rightarrow \pi^*$
[Fe(BMH*o*CB)$_2$]	618	234	$^5T_{2g} \rightarrow {}^5E_g$
[Co(BMH*o*CB)$_2$]	890	91	$^4T_{1g}(F) \rightarrow {}^4T_{2g}(F)$ (ν_1)
	696	547	$^4T_{1g} \rightarrow {}^4T_{2g}$ (ν_2)
	550	938	$^4T_{1g}(F) \rightarrow {}^4T_{2g}(P)$ (ν_3)
[Ni(BMH*o*CB)$_2$]	978	91	$^3A_{2g}(F) \rightarrow {}^3T_{2g}(F)$ (ν_1)
	685	331	$^3A_{2g}(F) \rightarrow {}^3T_{1g}(F)$ (ν_2)
	530	657	$^3A_{2g}(F) \rightarrow {}^3T_{1g}(P)$ (ν_3)
[Pd(BMH*o*CB)$_2$]	326	4589	MLCT
	245	7365	MLCT
[Cu(BMH*o*CB)$_2$]	875	12	$^2B_{1g} \rightarrow {}^2A_{1g}(d_{x2-y2} \rightarrow d^2_z)$ (ν_1)
	690	103	$^2B_{1g} \rightarrow {}^2B_{2g}(d_{x2-y2} \rightarrow d_{zy})$ (ν_2)
	475	196	$^2B_{1g} \rightarrow {}^2E_g(d_{x2-y2} \rightarrow d_{zy}, d_{yz})$ (ν_3)
[Ru(BMH*o*CB)$_3$]	625	245	$^2T_{2g} \rightarrow {}^4T_{1g}$
	430	6945	$^2T_{2g} \rightarrow {}^4T_{2g}$
	321	9784	$^2T_{2g} \rightarrow {}^2A_{2g}$, $^2T_{1g}$
[Rh(BMH*o*CB)$_3$]	550	1065	$^1A_{1g} \rightarrow {}^3T_{1g}$
	502	7894	$^1A_{1g} \rightarrow {}^1T_{1g}$
	425	8456	$^1A_{1g} \rightarrow {}^1T_{2g}$
[Ir(BMH*o*CB)$_3$]	642	106	$^1A_{1g} \rightarrow {}^3T_{1g}$
	470	794	$^2T_{2g} \rightarrow {}^4T_{2g}$
	391	7456	$^2T_{2g} \rightarrow {}^2A_{2g}$
[Cr(BMH*o*CB)$_3$]	570	1069	$^4A_{2g} \rightarrow {}^4T_{2g}$
	365	5891	$^4A_{2g} \rightarrow {}^4T_{1g}(F)$
[Mn(BMH*o*CB)$_2$]	560	978	$^6A_{1g} \rightarrow {}^4T_{1g}$ (^{4}G) (ν_1)
	399	2457	$^6A_{1g} \rightarrow {}^4E_g$ (^{4}G) (ν_2)
	345	3154	$^4A_{1g}$ (^{4}G) (10B+5C) $^6A_{1g} \rightarrow {}^4E_g$ (^{4}D) (ν_3)
	312	7488	(17B+5C), $^6A_{1g} \rightarrow {}^4T_{1g}$ (^{4}P) (ν_4)

2.2. ESR Spectra:

At ambient temperature, the Cu(II) complex's EPR spectra were captured on the X-Band at a frequency of 9.1 GHz with a magnetic field strength of 3400 G scan rate 2000. Splitting occurs in the solution phase, although the complex spectra only showed one broad anisotropic signal. The idea that the interaction between two paramagnetic centres is minimal can be used to explain why the band for the transition ΔMs = 2 is absent[35,36]. The spectra analysis yields two values for $g_{||}$ and $g_{\perp}$, 2.1035 and 2.0383, respectively. The observed $g_{\perp}$ value for the Cu(II) complexes is less than 2.3, consistent with the M-L bond's covalent nature. The unpaired electron is concentrated in the d_{x2-y2} orbital, according to the ratio $g_{||} > g_{\perp} > 2.0023$ determined for Cu(II) complexes, and the spectrum characteristics are typical of axial and tetragonally elongated geometry.

Table-3: EPR spectral data of the $[Cu(BMHoCB)_2]$ complexes

$g_{||}$	$g_{\perp}$	so	g
2.1035	2.0383	2.0582	2.0709

2.3. The FT(IR) spectra:

The FT(IR) spectra of the HBMH*o*CB ligand and its transition metal complexes scrutiny of observed data observed broadband at 3239 cm^{-1} due to the ν(-OH), of the HBMH*o*CB ligand, after complexation this band disappeared, indicated that this group participation in coordination[37-39]. The sharp bands of HBMH*o*CB ligand observed at 1556 and 1614 cm^{-1} were assigned to the oximino and azomethine groups. These bands were shifted to lower sites after complexation, suggesting that both groups participated in coordination[40-43]. For FT(IR, data of the transition metal complexes show non-ligand bands which can be assigned to ν(M-N) (oximino) (475-499 cm^{-1}) and ν(M→N) (azomethine) (501-525cm^{-1}) respectively[44-45].

Table-3: FT(IR) spectral bands of the ligand (HBMH*o*CB) and its metal complexes (cm^{-1}):

Assignments	HBMHoCB	Fe(II)	Co(II)	Ni(II)	Pd(II)	Cu(II)	Ru(III)	Rh(III)	Ir(III)	Cr(III)	Mn(II)
νOH Oximino	3378	-	-	-	-	-	-	-	-	-	-
νC=C Ar.	3022	3021	3017	3023	3020	3023	3016	3017	3021	3026	3021
νC=NN	1614	1591	1594	1589	1595	1593	1596	1598	1591	1594	1593
νC=NO	1556	1530	1533	1537	1538	1540	1539	1538	1539	1540	1540
νN-N	955	1001	1003	1008	1002	1005	1002	1001	1007	1004	1003
νN→O	-	985	957	965	922	956	978	977	969	974	966
νM-N	-	509	511	501	507	509	508	525	511	514	502
νM→N	-	483	477	475	475	479	499	493	475	491	493

2.4. PMR Spectra:

The PMR spectrum of ligand in d_6 DMSO solution exhibits an acidic peak at δ11.56ppm due to the -OH proton of the oximino group. The PMR spectrum of $[Pd(BMHoCB)_2]$complex reveals the absence of the proton signal due to the N-OH group, indicating that the proton signal due to oximino N-OH group is replaced on complexation with the Pd(II) metal ion. The ^1H NMR spectrum of HBMH*o*CB ligand and Pd(II), in DMSO–d_6 solvent, show a singlet signal at □8.54 ppm equivalent to the first proton assigned to =CH- group. The multiple signals at □7.27-7.70ppm are due to aromatic hydrogen of carbon of ligand and metal complexes.

Table-5: PMR spectral data of HBMH*o*CB ligand and its Pd(II) complexes

Compound	NOH	=CH-	Aromatic Proton
HBMHoCB	11.56	8.54	7.27-7.70
$[Pd(BMHoCB)_2]$	-	8.59	7.27-7.70

Antibacterial activity

Evaluations have been conducted between Schiff base HBMH*o*CB and its metal(II) complexes in terms of their antibacterial efficacy against G(+) and G(-) pathogens. The Minimal Inhibition Concentration (MIC) and the growth inhibition zone against test organisms were used to evaluate bactericidal activities. Antibacterial activity against *Escherichia coli*, *Staphylococcus aureus*, and *Klebsiella pneumoniae* was observed in the new metal complexes that were prepared. The nickel(II) compound has the highest bactericidal activity

against *S. aureus* and *E. coli* (MIC of 17 μg/ml) among the Schiff base coordination compounds produced. With a MIC against *E. coli* between 12.5 and 25 μg/ml, all complexes performed better than the gold standard, *Streptomycin*. Cobalt(II) and copper(II) compounds exhibited modest activity, but without significant MIC values, against Gram-negative bacteria (*P. aeruginosa* and *S. epidermidis*), while most of the other coordination compounds showed little or no activity. In general, chelation elevates the ligand's antibacterial potency. Coordination has been shown to increase the lipophilicity of the central metal atom in a complex, which can increase the likelihood of the metal diffusing across the cell membrane and disrupting metal-enzyme binding sites. However, our findings suggest that factors apart from membrane permeability must also play a role in determining bactericidal action.

3. Conclusion:

Thus, in light of the discussion from spectral and physicochemical analysis, the stereochemistry of the HBMH*o*CB ligand about the central trivalent metal ion is interesting and described in **Figure-2**. Based on physicochemical, the HBMH*o*CB ligand acts as a neutral bidentate coordinated through nitrogen atoms of azomethine and oximino groups.

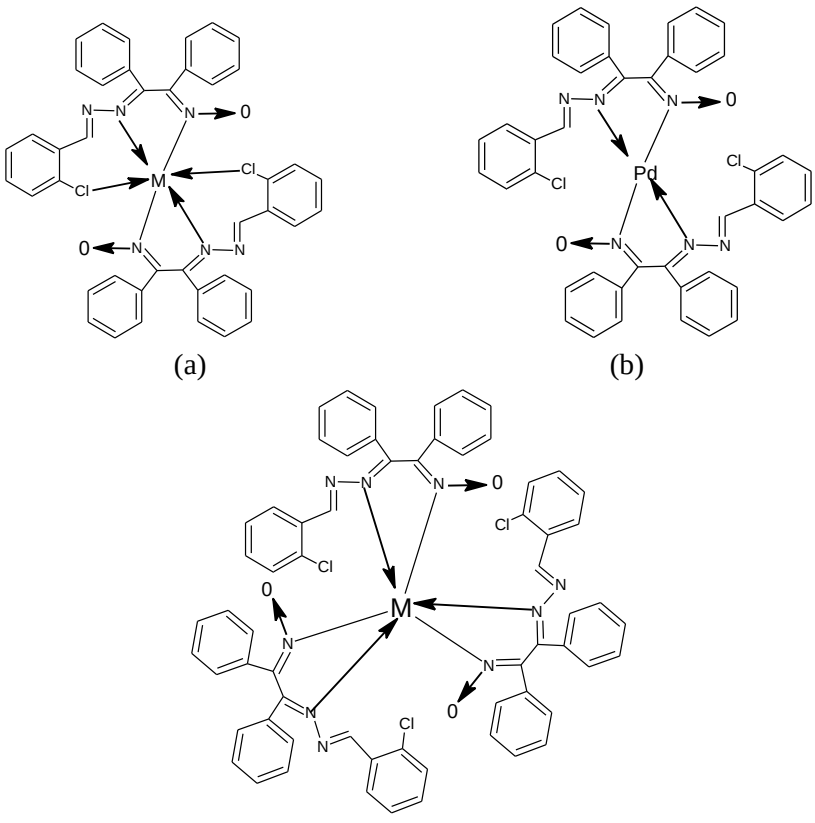

(a) (b) (c)

Where M = (a) Fe(II), Co(II), Ni(II), Cu(II), Mn(II) and (c) Rh(III), Ru(III), Cr(III), Ir(III)

Figure-2: Tentatively structures of the metal complexes

4. References:

1. Singh, M. S., & Narayan, P. (2001) . Complexes of titanium tetrachloride with benzilmonoxime and benzildioxime. Synthesis and Reactivity in Inorganic and Metal-Organic Chemistry, 31(1), 149–156. doi:10.1081/sim-100001940.
2. Eskandari, H., & Karkaragh, G. H. I. (2003). A Facile Spectrophotometric Method for Cobalt Determination Using. α-Benzilmonoxime in Sodium Dodecylsulfate Micellar Solutions. Analytical Sciences, 19(11), 1549–1552. doi:10.2116/analsci.19.1549.
3. Soleimani, E. (2012). Synthesis, spectral and thermal behaviour of two novel Cr(III) complexes with dibromobenziloxime. Journal of Thermal Analysis and Calorimetry, 111(1), 129–136. doi:10.1007/ s10973-012-2438-8.
4. Taylor, T. W. J., Callow, N. H., & Francis, C. R. W. (1939). 54. The metallic derivatives of hydrazones and the oxime-hydrazones of benzil. Journal of the Chemical Society (Resumed), 257. doi:10.1039/ jr9390000257.
5. Soleimani, E. (2010). Synthesis and Characterization of a Novel Benziloxime

Ligand and Its Iron(III) and Nickel(II) Complexes. Journal of the Chinese Chemical Society, 57(3A), 332–337. doi:10.1002 /jccs.20 1000049.

6. Soleimani, E. (2010). Novel Complexes of Mn(II), Co(II), and Cu(II) with Ligand Derived from Dibromobenziloxime. Journal of the Chinese Chemical Society, 57(4A), 653–658. doi:10.1002/jccs. 201000091.
7. Hay, R., Fraser, I., Reid, V. C., & Smith, C. (1994). The preparation of 12-, 13- and 14-membered tetra-imine macrocycles and characterisation of their copper(II) complexes. Transition Metal Chemistry, 19(3). doi:10.1007/bf00139100.
8. Ensafi, A. A., & Eskandari, H. (1999). Highly Selective Liquid–Liquid Extraction from Sulfuric Acid Medium and Spectrophotometric Determination of Palladium(II) with α-Benzilmonoxime. Microchemical Journal, 63(2), 266–275. doi:10.1006/mchj.1999.1790.
9. Eskandari, H., Ghaziaskar, H. S., & Ensafi, A. A. (2001). Solid–liquid separation after liquid–liquid extraction using α-benzilmonoxime-molten benzophenone for preconcentration and selective spectrophotometric determination of palladium. Analytical Letters, 34(14), 2535–2546. doi:10.1081/al-100107534.
10. Ahmed, A. H., Hassan, A. M., Gumaa, H. A., Mohamed, B. H., Eraky, A. M., & Omran, A. A. (2016). Copper(II)-oxaloyldihydrazone complexes: Physico-chemical studies: Energy band gap and inhibition evaluation of free oxaloyldihydrazones toward the corrosion of copper metal in acidic medium. Arabian Journal of Chemistry. doi:10.1016/j.arabjc.2016.05.015.
11. Urrutia, O., Erro, J., Guardado, I., San Francisco, S., Mandado, M., Baigorri, R., … Ma Garcia-Mina, J. (2013). Physico-chemical characterisation of humic-metal-phosphate complexes and their potential application to manufacture new types of phosphate-based fertilisers. Journal of Plant Nutrition and Soil Science, 177(2), 128–136. doi:10.1002/jpln. 201200651.
12. Ramadan, A. M., Alshehri, A. A., & Bondock, S. (2019). Synthesis, physicochemical studies and biological evaluation of new metal complexes with some pyrazolone derivatives. Journal of Saudi Chemical Society. doi:10.1016/j.jscs.2019.08.001.
13. Fouad, R., Shaaban, I. A., Ali, T. E., Assiri, M. A., & Shenouda, S. S. (2021). Co (ii), Ni (ii), Cu (ii) and Cd (ii)-thiocarbonohydrazone complexes: spectroscopic, DFT, thermal, and electrical conductivity studies. RSC advances, 11(60), 37726-37743. DOI: 10.1039/D1RA06902K.
14. Ahmed, A. H., & Moustafa, M. G. (2020). Spectroscopic, morphology and electrical conductivity studies on Co(II), Ni(II), Cu(II) and Mn(II)- oxaloyldihydrazone complexes. Journal of Saudi Chemical Society. doi:10.1016/j.jscs.2020.02.003.
15. Guzzi, S. A., & El Alagi, H. S. (2013). Synthesis and characterisation of Fe (II) and Co (II) Schiff base complexes derived from 3, 3′-diaminobenzidine and salicylaldehyde. J. Chem. and Pharm. Res, 5(10), 10-14.
16. Chandra, S., & Gupta, L. K. (2004). EPR and electronic spectral studies on Co(II), Ni(II) and Cu(II) complexes with a new tetradentate [N4] macrocyclic ligand and their biological activity. Spectrochimica Acta Part A: Molecular and Biomolecular Spectroscopy, 60(7), 1563–1571. doi:10.1016/j.saa.2003.08. 023.
17. Chandra, S., & Gupta, L. K. (2004). EPR, IR and electronic spectral studies on Mn(II), Co(II), Ni(II) and Cu(II) complexes with a new 22-membered azamacrocyclic [N4] ligand. Spectrochimica Acta Part A: Molecular and Biomolecular Spectroscopy, 60(8-9), 1751–1761. doi:10.1016/j.saa.2003.07.011.
18. Mojumdar, S. C., Miklovič, J., Krutošíková, A., Valigura, D., & Stewart, J. M. (2005). Furopyridines and furopyridine-Ni(II) complexes. Journal of Thermal Analysis and Calorimetry, 81(1), 211–215. doi:10. 1007/s10973-005-0769-4.
19. Nair, M. S., & Joseyphus, R. S. (2008). Synthesis and characterisation of Co(II), Ni(II), Cu(II) and Zn(II) complexes of tridentate Schiff base derived from vanillin and dl-α-aminobutyric acid. Spectrochimica Acta Part A: Molecular and Biomolecular Spectroscopy, 70(4), 749–753. doi:10.1016/ j.saa.2007.09.006.
20. El-Tabl, A. S. (2002). Transition Metal Chemistry,27(2),166–170. doi:10.1023/ a:1013952726823.
21. Chandra, S., & Kumar, U. (2005). Spectral and magnetic studies on manganese(II), cobalt(II) and nickel(II) complexes with Schiff bases. Spectrochimica Acta Part A: Molecular and Biomolecular Spectroscopy, 61(1-2), 219–224. doi:10.1016/j.saa.2004.03.036.

22. Gülcan, M., Sönmez, M., & Berber, İ. (2012). Synthesis, characterisation, and antimicrobial activity of a new pyrimidine Schiff base and its Cu (II), Ni (II), Co (II), Pt (II), and Pd (II) complexes. Turkish Journal of Chemistry, 36(1), 189-200.
23. El-Asmy, A. A., & Al-Hazmi, G. A. A. (2009). Synthesis and spectral feature of benzophenone-substituted thiosemicarbazones and their Ni(II) and Cu(II) complexes. Spectrochimica Acta Part A: Molecular and Biomolecular Spectroscopy, 71(5), 1885–1890. doi:10.1016/j.saa.2008.07.005.
24. Rakha, T. H., El-Gammal, O. A., Metwally, H. M., & Abu El-Reash, G. M. (2014). Synthesis, characterisation, DFT and biological studies of(Z)-N′-(2-oxoindolin-3-ylidene) picolinohydrazide and its Co(II), Ni(II) and Cu(II) complexes. Journal of Molecular Structure, 1062, 96–109. doi:10.1016/j. mol struc.2013.12.086.
25. Chandra, S., Raizada, S., Tyagi, M., & Sharma, P. K. (2008). The spectroscopic and biological approach of Ni(II) and Cu(II) complexes of 2-pyridine carboxaldehyde thiosemicarbazone. Spectrochimica Acta Part A: Molecular and Biomolecular Spectroscopy, 69(3), 816–821. doi:10.1016/j.saa.2007.05.033.
26. Ejidike, I. P., & Ajibade, P. A. (2016). Synthesis,Characterization,Anticancer, and Antioxidant Studies of Ru(III) Complexes of Monobasic Tridentate Schiff Bases. Bioinorganic Chemistry and Applications, 2016, 1–11. doi:10.1155 /2016 /9672451.
27. Abouzayed, F. I., Emam, S. M., & Abouel-Enein, S. A. (2020). Synthesis, characterisation and biological activity of nano-sized Co(II), Ni(II), Cu(II), Pd(II) and Ru(III) complexes of tetradentate hydrazone ligand. Journal of Molecular Structure, 128314. doi:10.1016/j.molstruc.2020.128314.
28. Anan, N. A., Hassan, S. M., Saad, E. M., Butler, I. S., & Mostafa, S. I. (2011). Preparation, characterisation and pH-metric measurements of 4-hydroxysa licyli denechitosan Schiff-base complexes of Fe(III), Co(II), Ni(II), Cu(II), Zn(II), Ru(III), Rh(III), Pd(II) and Au(III). Carbohydrate Research, 346(6), 775–793. doi:10.1016/j.carres.2011.01.014.
29. Mukhopadhyay, S., Gupta, R. K., Paitandi, R. P., Rana, N. K., Sharma, G., Koch, B., … Pandey, D. S. (2015). Synthesis, Structure, DNA/Protein Binding, and Anticancer Activity of Some Half-Sandwich Cyclometalated Rh(III) and Ir(III) Complexes. Organometallics, 34(18), 4491–4506. doi:10. 1021/acs. organomet.5b00475.
30. Ma, D., Tsuboi, T., Qiu, Y., & Duan, L. (2016). Recent Progress in Ionic Iridium(III) Complexes for Organic Electronic Devices. Advanced Materials, 29(3), 1603253. doi:10.1002/adma.201603253.
31. Scott, N. M., Dorta, R., Stevens, E. D., Correa, A., Cavallo, L., & Nolan, S. P. (2005). Interaction of a BulkyN-Heterocyclic Carbene Ligand with Rh(I) and Ir(I). Double C−H Activation and Isolation of Bare 14-Electron Rh(III) and Ir(III) Complexes. Journal of the American Chemical Society, 127(10), 3516–3526. doi:10.1021/ja043249f.
32. Brahim, H., & Daniel, C. (2014). Structural and spectroscopic properties of Ir(III) complexes with phenyl pyridine ligands: Absorption spectra without and with spin–orbit-coupling. Computational and Theoretical Chemistry, 1040-1041, 219–229. doi:10.1016/j.comptc.2014.01.030.
33. Singh, D. P., Kumar, R., & Singh, J. (2009). Synthesis and spectroscopic studies of biologically active compounds derived from oxalyldihydrazide and benzil, and their Cr(III), Fe(III) and Mn(III) complexes. European Journal of Medicinal Chemistry, 44(4), 1731–1736. doi:10.1016/j.ejmech .2008.03.007.
34. Chandra, S., & Sharma, S. D. (2002) . Transition Metal Chemistry, 27(7), 732–735. doi:10.1023/a: 10203 09322470.
35. B. Jezowska, J. Lisowski, A. Vogt, P. Chemielewski, Polyhedron 7 (1988) 1053.
36. P.P. Hankare, S.S. Chavan, Ind. J. Chem. 42A (2003) 540.
37. Fedaoui D, Bouzina A, Aouf N, Bouhadja Y and Berredjem M; Synthesis, characterisation and spectroscopic studies of iron(III) and copper(II) complexes of α-hydroxyl phosphonate; Der Pharma Chemica; **2016**, 8(1), 124-127.
38. Gholamreza K, Marteza M and Nasrin H; Manganese (II)-bis(Salicyaldehyde)-4-methyl-1, 2-phenylenediamines (Mn-BSMP) as an inexpensive N_2O_2 type Schiff base catalyst for oxidative decarboxylation of carboxylic acids with (n-Bu_4NIO_4) in the presence of imidazole; Iran J Chem. Engg; **2011**, 30(4), 13-18.
39. Raja K, Gandhi N, Lekha L, Easwaramoorthy D and catalytic properties of Ru(III) Schiff

base complexes containing N, O donors; J of Mole Str; **2014**, 1060, 49-57.
40. Nemade A, Patil K and Kolhe V; Synthesis, composition and spectral studies of some transition metal complexes with 3-aminolawsonoxime; Res J Chem Sci; **2017**, 7(1), 25-31.
41. Joshi S and Habib S; Co(II) and Zn(II) metal complexes of heterocyclic Schiff bases: a Synthesis, spectral and antimicrobial study; Ori J of Chem; **2014**, 30(3), 1343-1348.
42. Balashova T and Fukin G; Lanthanide complexes with the Schiff base containing sterically hindered phenol: Synthesis, structure and luminescence properties; Russs J of Coord Chem; **2017**, 43(12), 852-857.
43. Al-Hamdani A, Mahmoud M and Bakir S; Synthesis, structural studies of some new transition metals complexes of semicarbazide hydro-chloride Schiff base derivatives; **2013**, 1(3), 583-596.
44. Sumathi R and Halli M; Metal (II) complexes derived from naphthofuran-2-carbohydrazide and diacetylmonoxime Schiff base; Synthesis, spectroscopic, electrochemical and biological investigation; Bioinorg Chem and Appl; **2014**, 1-11.
45. Alsaygh A, Al-humid J and Najjar I; Iridium (III) hydrocyclometallated-imine complexes, as a result of C-H bond activation in coordinated ligand, spectroscopic studies; Asian J of Sci and Tech; **2014**, 5(11), 647-652.